

COMPARISON BETWEEN THE PITTING CORROSION OF PURE Al AND Al-Si ALLOYS IN DEAERATED NEUTRAL SODIUM PERCHLORATE SOLUTIONS AND THE EFFECT OF SOME INORGANIC INHIBITORS

Omar Abdullah Hazzazi *

Department of Chemistry, Faculty of Applied Science, Umm Al-Qura University,
P.O.Box 2897, Makkah, Saudi Arabia

الخلاصة:

يُعنى هذا البحث بمقارنة التآكل الثقبي للألمنيوم النقي في محاليل متعادلة من فوق كلورات الصوديوم وبعض سبائك الألمنيوم-سيلكون في نفس المحاليل تحت نفس الظروف. ولقد استُخدمت في هذا البحث سبيكة (ألمنيوم + 6 % سيلكون) وسبيكة (المنيوم + 12 % سيلكون) وسبيكة (ألمنيوم + 18 % سيلكون). وقد أُختبرت هذه السبائك لما لها من تطبيقات متعددة في الصناعة تفوق- في بعض المجالات - تطبيقات الألمنيوم النقي. وقد تمت الدراسة باستخدام الاستقطاب البوتنشيوديناميكي ومنحنيات الجهد مع الزمن عند تيارات ثابتة. وأظهرت الدراسة أن منحنيات الاستقطاب البوتنشيوديناميكي لكل العينات لا يوجد فيها منطقة نشاط بسبب وجود طبقة خمول من أكسيد الألومنيوم على سطح الفلز. ويتبع منطقة الخمول ارتفاع ملحوظ في التيار عند جهد حرج يسمى جهد كسر طبقة الخمول (E_b) نتيجة لكسر طبقة الخمول بوساطة أنيونات فوق الكلورات. وقد تم في هذا البحث تفسير ميكانيكية كسر طبقة الخمول بوساطة أنيون فوق الكلورات بطريقة أعم وأشمل مما جاء في البحث رقم 13. وقد لوحظ أن زيادة تركيز أنيون فوق الكلورات يؤدي إلى إزاحة قيم (E_b) إلى الاتجاه السالب (الاتجاه النشط) مما يعني نقص مقاومة الطبقة الخاملة للتآكل، بينما تتجه قيم (E_b) إلى الاتجاه الموجب (الاتجاه الخامل) كلما زادت نسبة السيلكون في العينة، مما يعني زيادة مقاومة الطبقة الخاملة للتآكل الثقبي بزيادة نسبة السيلكون في العينة، حيث وُجد أن مقاومة سبيكة (ألمنيوم + 18 % سيلكون) للتآكل الثقبي تفوق مقاومة سبيكة (ألمنيوم + 12 % سيلكون) والأخيرة تفوق مقاومة سبيكة (الومنيوم + 6 % سيلكون) التي بدورها تفوق مقاومة الألمنيوم للتآكل الثقبي. من هنا يظهر الهدف الرئيسي من هذا البحث وهو التركيز على توضيح دور السيلكون في رفع مقاومة الألمنيوم لهذا النوع الخطير من التآكل. وبدراسة منحنيات الجهد مع الزمن عند تيارات ثابتة لوحظ أن الجهد يزداد في البداية مع الزمن حتى يصل إلى قيمة ثابتة عند زمن معين يسمى بزمن الحضانة (ويُعزى ذلك إلى تكوين الطبقة الخاملة فوق سطح القطب)، ويقطع بعد ذلك نتيجة كسر الطبقة الخاملة وبداية التآكل الثقبي. وقد لوحظ أن زمن الحضانة يقل (وبالتالي يزداد معدل التآكل) بزيادة كثافة التيار و تركيز أنيون فوق الكلورات، بينما يزداد زمن الحضانة (و بالتالي يقل معدل التآكل) بزيادة نسبة السيلكون في العينة. وقد تم في هذا البحث أيضاً دراسة تأثير إضافة أنيونات الموليبدات والتنجستات، كمثبطات غير عضوية الى محلول فوق كلورات الصوديوم على التآكل الثقبي للألمنيوم وسبائك الألمنيوم-سيلكون.

* E-mail: hazazi@hotmail.com

ABSTRACT

This paper reports the results of potentiodynamic polarization and chronopotentiometry potential/time measurements on the pitting corrosion of pure Al and three Al–Si alloys, namely (Al + 6% Si), (Al + 12% Si), and (Al + 18% Si) in deaerated neutral sodium perchlorate solutions, complemented by *ex situ* energy dispersive X-ray (EDX) examinations of the electrode surface. In all cases, the potentiodynamic anodic polarization curves do not exhibit an active dissolution region due to spontaneous passivation. The passivity is due to the presence of a thin film of Al_2O_3 on the anode surface. The passive region is followed by pitting corrosion as a result of breakdown of the passive film by ClO_4^- ions. Polarization measurements showed that the breakdown potential (E_b) decreases with increase in ClO_4^- concentration, while it increases with increasing %Si in the alloy. The resistance of the four tested samples towards pitting corrosion increases in the order: $\text{Al} < (\text{Al} + 6\% \text{ Si}) < (\text{Al} + 12\% \text{ Si}) < (\text{Al} + 18\% \text{ Si})$. Chronopotentiometry potential/time measurements show that the incubation time for pitting initiation decreases with increasing ClO_4^- concentration and applied anodic current density, while it increases with increasing Si content in the alloy. Addition of WO_4^{2-} and MoO_4^{2-} , as inorganic inhibitor anions, to the perchlorate solution inhibits pitting corrosion to an extent depending on the concentration and type of the added inhibitor.

Key words: pitting corrosion, Al; Al–Si alloys; sodium perchlorate solutions

COMPARISON BETWEEN THE PITTING CORROSION OF PURE Al AND Al-Si ALLOYS IN DEAERATED NEUTRAL SODIUM PERCHLORATE SOLUTIONS AND THE EFFECT OF SOME INORGANIC INHIBITORS

1. INTRODUCTION

The many important applications of Al and Al alloys have resulted in research into their electrochemical behavior and corrosion inhibition in a wide variety of media. The breakdown of the passive oxide films on Al and its alloys, by aggressive anions such as halides at sufficiently positive anodic potentials is frequently responsible for the failure of Al and its alloys in aqueous halide solutions, because it usually leads to severe pitting of the underlying metal [1–12]. Literature survey showed that little seems to have been published concerning pitting corrosion of Al and its alloys in perchlorate solutions. Recently, Mohammed *et al.* [13] studied the pitting corrosion behavior of pure Al in aerated neutral sodium perchlorate solutions using AC and DC techniques. According to literature survey, except reference [13], nothing seems to have been published concerning pitting corrosion of Al-Si alloys in perchlorate solutions.

For these reasons, the main objective of the present work is to investigate the pitting corrosion behavior of three Al-Si alloys, namely (Al + 6% Si), (Al + 12% Si) and (Al + 18% Si) alloys, in deaerated neutral NaClO₄ solutions. Some experiments have also been carried out for pure Al in deaerated neutral NaClO₄ solutions with the aim to make a comparison between pitting corrosion of pure Al and Al-Si alloys in these solutions. The experiments were performed using potentiodynamic and galvanostatic measurements under the influence of various experimental conditions. It was also the purpose of the present work to study the effect of adding some inorganic inhibitors, such as sodium molybdate and sodium tungstate to perchlorate solution on the pitting corrosion of Al and Al-Si alloys. Some EDXA examinations of the electrode surface have been carried out.

2. EXPERIMENTAL

2.1. Solutions

The electrolytes employed in this study were sodium perchlorate, NaClO₄, (the pitting corrosion agent) and two inorganic inhibitors, namely sodium molybdate (Na₂MoO₄) and sodium tungstate (Na₂WO₄). All these electrolytes were purchased from Merck (Darmstadt, Germany). The electrolytes were prepared using analytical grade reagents (Merck) and triply distilled water. Sodium perchlorate was dissolved in triply distilled water at concentrations in the range of (0.05–1.0 M). The two inorganic inhibitors were dissolved at concentrations in the range of (0.001–0.01) in 0.50 M NaClO₄ solutions. All solutions were sparged with Ar gas for 45 min. prior to use. Ar bubbling was stopped to prevent convection effects and the argon blanket was maintained over the solution throughout the experiment. The electrode was then immediately immersed in the test solution. The solution temperatures were adjusted to the required values ($\pm 1^\circ\text{C}$), using a water thermostat.

2.2. Electrodes and Apparatus

Four working electrodes were used in this work; very pure Al rod (99.99 % Koch Light Laboratories, Colnbrook Bucks, UK) and three (Al-xSi) alloys; $x = 6, 12,$ and 18% . Experiments were carried out in a three-compartment glass cell. Electrode potentials were measured and reported against the external saturated calomel electrode with NaCl solution. A platinum wire was used as an auxiliary electrode. Reference and auxiliary electrodes were individually isolated from the test solution by glass frits. For electrochemical measurements, the investigated materials were cut as cylindrical rods, welded with Cu-wire for electrical connection and mounted in glass tubes of appropriate diameter using Araldite to offer an active flat disc shaped surface of (0.50 cm²) geometric area, to contact the test solution. Prior to each experiment, the working electrodes were mechanically polished with aluminum powders of different grain sizes down to 0.05 μm , using water as lubricant, and was then repeatedly rinsed with water, dried, and then etched in a 0.10 M NaOH solution for 30 s. The etched electrode was rinsed with deionized water rapidly, followed by immediate rinsing with absolute ethanol. The aim of using the NaOH etching method was to produce a fresh and active (oxide-free) electrode surface as much as possible. The experiments were carried out in deaerated solutions of different concentrations (0.05 – 1.0 M) of NaClO₄. Other experiments have been carried out in 0.50 M NaClO₄ solution containing various concentrations of Na₂MoO₄ and Na₂WO₄ solutions at the required temperature ($\pm 1^\circ\text{C}$).

Potentiodynamic current/potential experiments were carried out at a scan rate of 1.0 mV s⁻¹. Chronopotentiometry potential/time measurements were carried out at a given anodic current density (j_a) at which the potential/time transient was recorded. A Potentiostat / Galvanostat (EG&G model 273) and a personal computer were used. M352 corrosion

software from EG&G Princeton Applied Research was used for potentiodynamic polarization and chronopotentiometry measurements.

The composition of the passive oxide film grown on the surface of Al as an example, in 0.50 M NaClO₄ solutions in the absence and presence of 0.05 M Na₂MoO₄ and Na₂WO₄, was tested by EDX examinations using a Traktor TN-2000 energy dispersive spectrometer. For EDX examinations, the samples were submitted to the same surface treatment previously mentioned, then immersed for 5 min in electrolytic solution at 25 °C under potentiostatic regime at a given potential within the potential range of the passive region, and finally washed thoroughly and submitted to 5 min of ultrasonic cleaning in order to remove loosely adsorbed ions.

3. RESULTS AND DISCUSSION

3.1. Polarization Measurements

3.1.1. Polarization Behavior of Al and the Three Al-Si Alloys in 0.50 M Deaerated Perchlorate Solutions

The potentiodynamic curves shown in Figure 1 demonstrates the overall polarization behavior recorded for pure Al and the three Al-Si alloys in 0.50 M deaerated NaClO₄ solution as a function of the applied potential. Potentials were swept starting from the corrosion potential of each electrode towards anodic direction at a scan rate of 1.0 mV s⁻¹ and at 25 °C. Before each polarization experiment, the electrode was allowed to corrode freely for a period of 120 min, then a steady state open circuit potential, OCP, corresponding to the corrosion potential (E_{corr}) of the working electrode, was obtained. Potential sweep was started from the corrosion potential in order to avoid the problem of the reduction of perchlorate ions to Cl⁻ ions [14]. It is obvious from Figure 1 that, in all cases, the manifestation of passivity persists as the potential is increased to a value exceeding a certain critical potential value, known as the breakdown potential (E_b). The relative insensitivity of current to increasing potential (characteristic of the passive region) changes abruptly as passivity breaks down at E_b , where a strong potential dependence of the current emerges and stable pitting ensues. The values of E_b have been found to depend on the composition of the tested Al samples, where E_b values move towards more anodic (noble) direction as Si content in the alloy is increased. These results lead to a general conclusion that the resistance of the tested samples towards pitting corrosion, caused by aggressive attack of ClO₄⁻ ions, increases with increasing %Si in the Al samples.

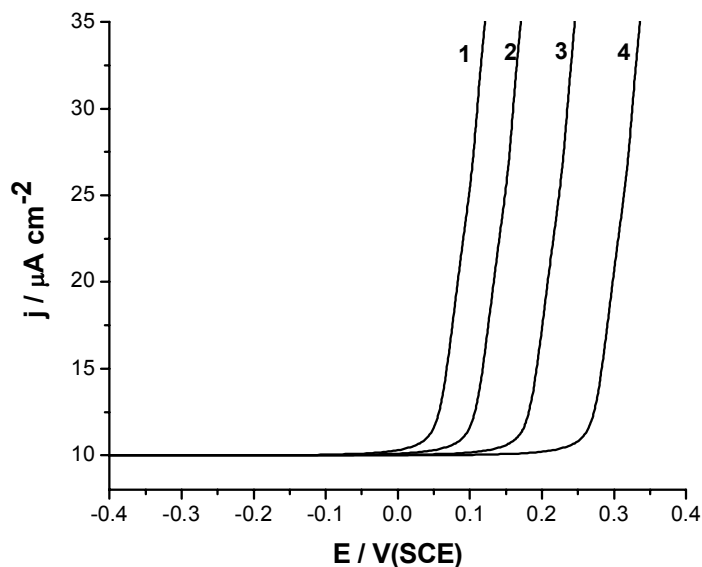


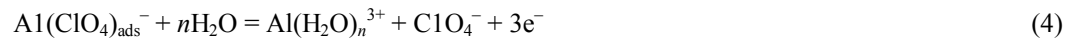
Figure 1. Potentiodynamic anodic polarization curves of Al, (Al + 6% Si), (Al + 12% Si), and (Al + 18% Si) alloys in 0.50 M NaClO₄ deaerated solution at a scan rate of 1.0 mV s⁻¹ and at 25 °C. (1) Al; (2) (Al + 6% Si) alloy; (3) (Al + 12% Si) alloy; (4) (Al + 18% Si) alloy

3.1.2. Mechanism of Passive Layer Formation and Passivity Breakdown

Further inspection of Figure 1 reveals that the anodic excursion span of all tested Al samples does not exhibit an active dissolution region near the corrosion potential (E_{corr}). The lack of active dissolution could be attributed to the spontaneous passivation of Al. Passivity is due to the presence of an Al_2O_3 film on the electrode surface [13, 15]. These results demonstrate that the oxide film is stable at and near E_{corr} . The passive oxide film formation could be explained on the basis that in deaerated neutral solutions, the main passivating (film forming) species are OH^- ions. These adsorb on the metal surface and promote repassivation following Equations (1) and (2)



where Equation 1 refers to a charge-transfer reaction. In the presence of ClO_4^- ions, there is a competition between OH^- ions (essential for passive film formation) and ClO_4^- ions (essential for passivity breakdown), for adsorption sites on the metal surface, consistent with Kruger's [16] adsorbed ion displacement model of passivity breakdown. The adsorption of ClO_4^- ions leads to local dissolution, as shown in Equations (3) and (4)



where Equation (4) is the dissolution step and $\text{Al}(\text{H}_2\text{O})_n^{3+}$ represents the solvated Al^{3+} ion. If the rates of reactions (1) and (2) are faster than those of (3) and (4), film healing processes predominate. The converse causes local dissolution (pitting) to dominate. If ClO_4^- ions adsorb strongly on Al surfaces to promote dissolution, as implied by Equations (3) and (4), then these species may be expected to remain bound to the solvated ion to form a soluble complex species, $\text{Al}(\text{ClO}_4)_{3(\text{aq})}$.



Formation of a soluble complex species plays an important role in the pitting corrosion process of Al [17]. The onset of pitting (E_{pit}) is now seen to arise as a simple consequence of the dissolution reactions (Equations 3 and 4) and subsequent formation of soluble complex species (Equation (5)) dominating over the film forming reactions (Equations (1) and (2)) at the base of the flaw, resulting in pits formation. Galvele *et al.* [18] demonstrated that electrochemical processes inside the pit are under mass-transfer control. The increased concentration of cations, due to metal dissolution, inside the pit leads to changes in localized solution chemistry. First, following Galvele [18], hydrolysis occurs to lower the pH, as represented by the general reaction in Equation 6



where $x = 1$ in the resulting acid solution. A second effect arises from the well-recognized requirement that electrical neutrality must be maintained throughout the electrolyte. Therefore, aggressive ClO_4^- anions must migrate into the pit to compensate for the local increase in cation concentration, as shown by the theoretical analysis of Ateya and Pickering [19]. This leads to an increase in ClO_4^- concentration in the pit. The overall effect of the pit initiation process is to produce a micropit at the base of the flaw with a local solution chemistry that is enriched in ClO_4^- and H^+ species. This causes a greater imbalance between the film-forming reactions and the dissolution reactions. Consequently, the pit once initiated continues to propagate and enlarge.

3.1.3. Effect of Perchlorate Concentration

The effect of perchlorate concentration on the potentiodynamic anodic polarization responses of pure Al and the three Al-Si alloys has been studied. Figure 2 presents the polarization data recorded for (Al + 12% Si) alloy at 25 °C. Similar results were obtained for pure Al and the other two Al-Si alloys. Figure 3 represents the relationship between E_b , recorded for Al and the three Al-Si alloys, and perchlorate concentration. Inspection of the data of Figures 2 and 3 reveals that for all samples, an increase in ClO_4^- concentration shifts E_b towards more negative (active) direction corresponding to decreased resistance to pitting corrosion. It follows from the data of Figure 4 that at a given ClO_4^- concentration, the values of E_b decrease in the order: (Al + 18% Si) > (Al + 12% Si) > (Al + 6% Si) > Al, indicating that the pitting corrosion resistance of the four samples decreases in the same sequence. It seems that the presence of Si, as an alloying element, increases the corrosion resistance of (Al-Si) alloys. This increase in the corrosion resistance of (Al-Si) alloys is enhanced by increasing the Si content in the alloy.

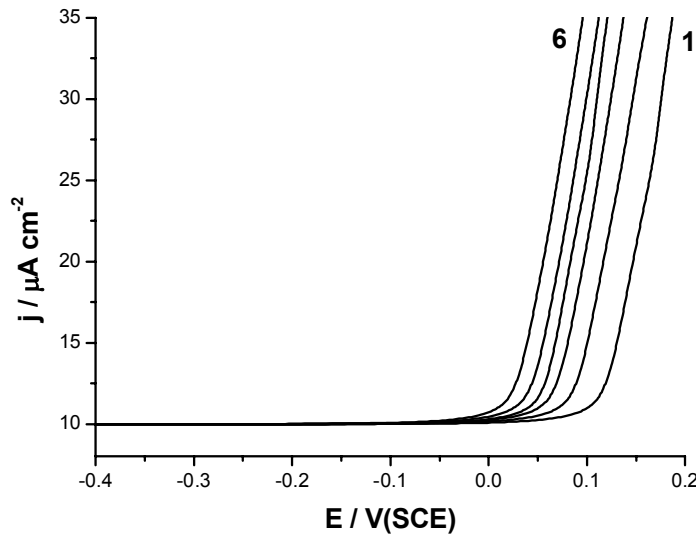


Figure 2. Potentiodynamic anodic polarization curves of pure Al in various concentrations of NaClO₄ solutions (0.05 – 1.0 M) at a scan rate of 1.0 mV s⁻¹ and at 25 °C. (1) 0.05 M; (2) 0.10 M; (3) 0.25 M; (4) 0.50 M; (5) 0.75 M; (6) 1.0 M

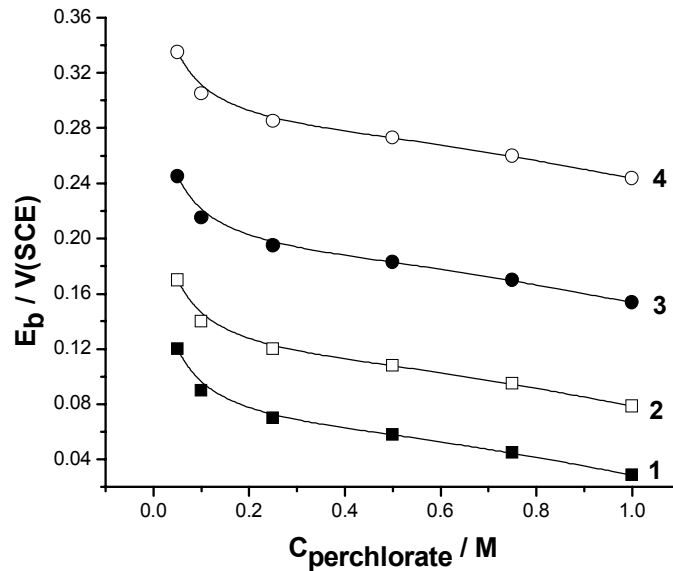


Figure 3. Dependence of the breakdown potential (E_b) on perchlorate concentration for Al and the three (Al–Si) alloys in various concentrations of NaClO₄ solutions at 25 °C. (1) Al; (2) (Al + 6% Si) alloy; (3) (Al + 12% Si) alloy; (4) (Al + 18% Si) alloy

3.1.4. Effect of Si Content in the Al–Si Alloys

It was concluded from the previous section that alloying Al with Si increases its resistance towards pitting corrosion in aggressive perchlorate solutions. The main objective of this section is to clarify the role played by Si in enhancing the pitting corrosion resistance of (Al–Si) alloys in these solutions. It is probable that any localized dissolution will preferentially dissolve Al and leave the surface enriched in unreactive Si atoms. Enrichment of alloy surface in unreactive Si atoms during dissolution blocks the active sites available for Al dissolution. At this stage, dissolution is retarded and pitting ceases. In order for pitting to recommence, the potential must be raised even higher (to $(E_{pit})_{alloy}$) to activate dissolution at the less favourable sites. As the Si content is increased, Si atoms will appear with greater frequency. Therefore, dissolution processes will be retarded until increasingly higher potentials are reached. Therefore, $(E_{pit})_{alloy}$ must increase with Si content, as shown in Figure 4. Other research workers attributed the high corrosion resistance of Al–Si alloys to the incorporation of Si atoms in the Al₂O₃ passive film [20]. This incorporation adjusts the film defects and precludes significant dissolution of the oxide film [21].

3.1.5. Effect of Inorganic Inhibitors

Figures 4 and 5 show, respectively, the effect of adding various concentrations of MoO_4^{2-} and WO_4^{2-} ions on the potentiodynamic polarization curves of (Al + 12%Si) alloy in 0.50 M NaClO_4 solution at a scan rate of 1.0 mV s^{-1} and at 25°C . Similar results were obtained for the other Al samples. The data clearly show that the presence of either MoO_4^{2-} or WO_4^{2-} ions in the aggressive perchlorate solution drifts E_b towards more anodic potentials (noble direction) and inhibits pitting corrosion of these samples [22]. The inhibiting effect of these inhibitors increases with their concentrations, as shown in Figure 6 (as an example). Plots similar to Figure 6 were obtained for the other Al samples. The higher values of E_b in the presence of WO_4^{2-} ions than those in the presence of MoO_4^{2-} ions suggest that WO_4^{2-} ions are more effective than MoO_4^{2-} ions in the inhibition of pitting corrosion of Al samples. The inhibiting function of the two inhibitors may be due to the reduction of Mo^{6+} in MoO_4^{2-} and W^{6+} in WO_4^{2-} , respectively, during film formation [23–25]. The reduction products (MoO_2 and WO_2 , respectively) help in adjusting the defects and preclude dissolution of the oxide film by ClO_4^- ions (see the details of Section 3.3). Consequently, these processes aid stability of the passive film such that pitting is inhibited. Moreover, it is probable that MoO_4^{2-} and WO_4^{2-} ions compete with ClO_4^- ions for surface adsorption sites [21–23], and consequently suppress the adsorption and incorporation of ClO_4^- ions into the passive film, thereby reducing the pitting susceptibility.

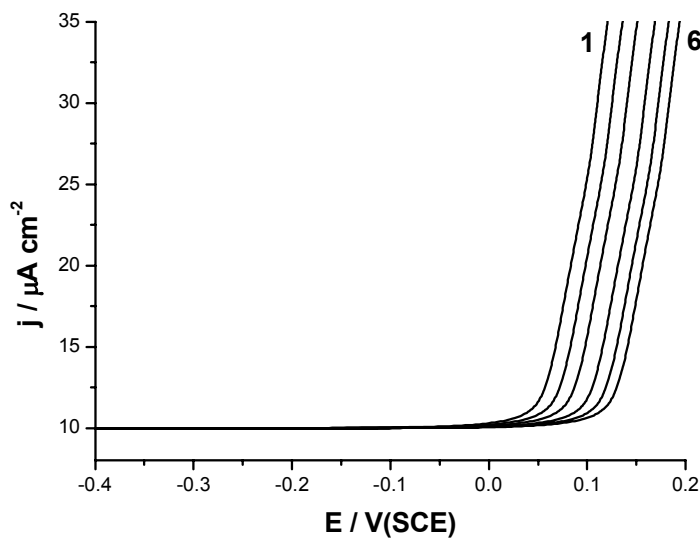


Figure 4. Potentiodynamic anodic polarization curves of pure Al in 0.50 M NaClO_4 solution in the absence and presence of various concentrations (0.001 – 0.01) of Na_2MoO_4 at a scan rate of 1.0 mV s^{-1} and at 25°C . (1) Blank; (2) 0.001 M; (3) 0.002 M; (4) 0.004 M; (5) 0.008 M; (6) 0.01 M

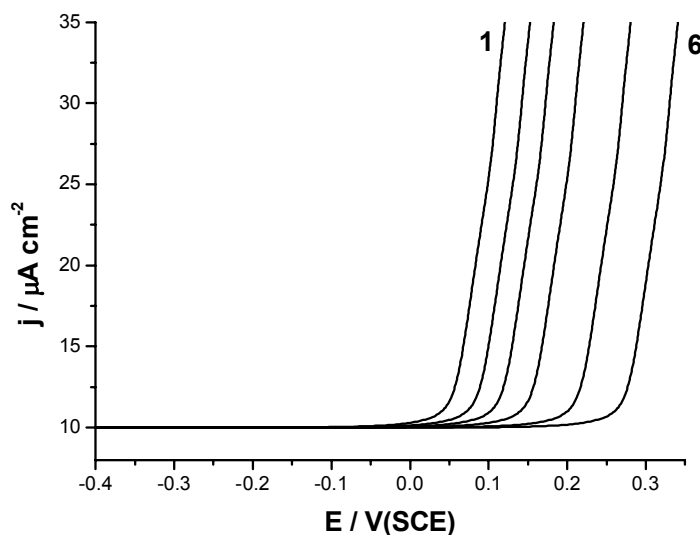


Figure 5. Potentiodynamic anodic polarization curves of pure Al in 0.50 M NaClO_4 solution in the absence and presence of various concentrations (0.001 – 0.01) of Na_2WO_4 at a scan rate of 1.0 mV s^{-1} and at 25°C . (1) Blank; (2) 0.001 M; (3) 0.002 M; (4) 0.004 M; (5) 0.008 M; (6) 0.01 M

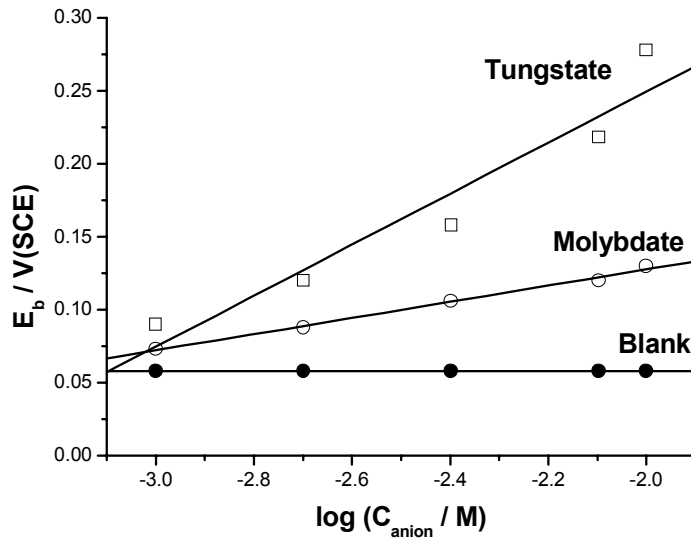


Figure 6. Relationship between the breakdown potential (E_b) and the logarithmic concentration of WO_4^{2-} and MoO_4^{2-} anions ($\log C_{anions}$) for Al in 0.50 M NaClO₄ solution at 25 °C

3.2. Chronopotentiometry Potential/Time Measurements

3.2.1. Effect of Perchlorate Concentration

Figure 7 shows the potential/time transients recorded for Al and the three (Al–Si) alloys in 0.50 M NaClO₄ solution at a current density (j_a) of 0.10 mA cm⁻² and at 25 °C. Potential/time transients of (Al + 12% Si) alloy in NaClO₄ solutions of different concentrations (0.05 –1.00 M) at 25 °C and current density $j_a = 0.10$ mA cm⁻² are given in Figure 8. Similar plots were recorded for the three alloys. It is obvious that in all cases, the anodic potential rises linearly with time reaching a maximum at a certain critical breakdown potential, E_b , corresponding to a characteristic pitting time parameter, known as the incubation time (t_i) [26, 27]. The incubation time is the time required for the aggressive anion (ClO₄⁻ ion in this study) to break down and penetrate the passive layer and reach the base metal. This linear increase in the anodic potential with time is undoubtedly due to thickening and growth of the passive layer on the electrode surface.

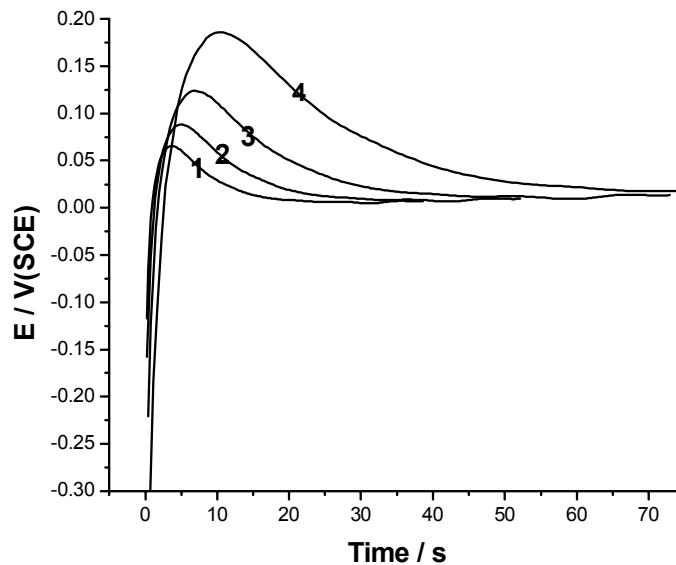


Figure 7. Potential/time transients recorded for Al and the three (Al–Si) alloys in 0.50 M NaClO₄ solution at a current density (j_a) of 0.10 mA cm⁻² and at 25 °C. (1) Al; (2) (Al + 6% Si) alloy; (3) (Al + 12% Si) alloy; (4) (Al + 18% Si) alloy

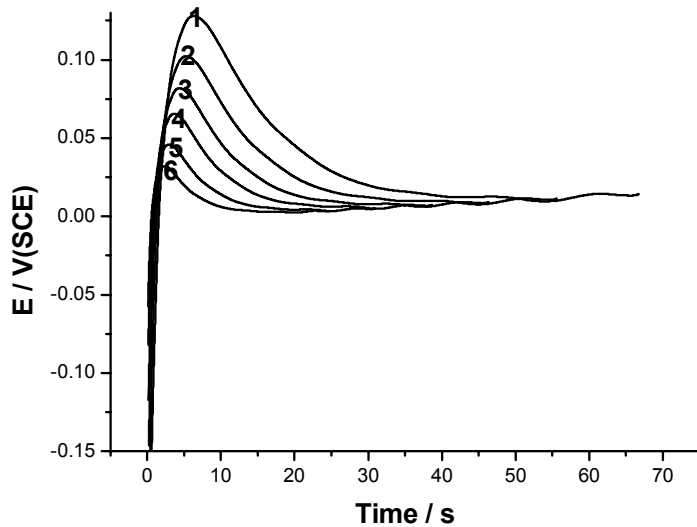


Figure 8. Potential–time transients recorded for pure Al in NaClO_4 solutions of different concentrations (0.05 – 1.0 M) at 25°C and at a current density of 0.10 mA cm^{-2} . (1) 0.05 M NaClO_4 ; (2) 0.10 M; (3) 0.25 M; (4) 0.50 M; (5) 0.75 M; (6) 1.00 M

The slope of this linear part, namely $(dE/dt)_{ja}$ represents the rate of passive layer growth [28, 29]. After t_i , the potential decreases with time as a result of pit growth, denoting passivity breakdown and initiation of pitting corrosion. Finally, the potential reaches a steady state value at almost 50 mV. The steady state potential may be attributed to stabilization of pitting process. It follows from the data of Figure 8 that an increase in ClO_4^- concentration decreases the slope of the linear part, and hence decreases the rate of film growth, as a result of thinning of the passive layer. In addition, increasing perchlorate concentration obviously decreases E_b and t_i . These results confirm those obtained from polarization measurements that the rate of pitting corrosion for all samples is enhanced with an increase in perchlorate concentration. To shed more light on this point, Figure 9 was constructed, and it shows the dependence of the rate of pit growth, defined as $(1/t_i)$, on the ClO_4^- concentration for the four samples. It is obvious from Figure 9 that for all of the samples, the rate of pit growth increases with an increase in perchlorate concentration. On the other hand, at a given perchlorate concentration, the rate of pit growth increases in the order: (Al + 18% Si) < (Al + 12% Si) < (Al + 6% Si) < Al, indicating that the pitting corrosion resistance of the four samples decreases in the same sequence. These results confirm the results obtained from polarization measurements that the presence of Si, as an alloying element, increases the pitting corrosion resistance of (Al–Si) alloys.

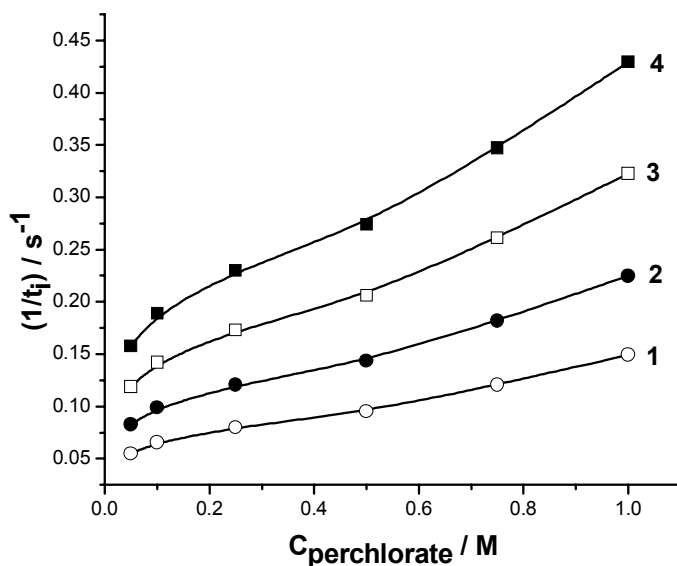


Figure 9. The dependence of the rate of pit growth (t_i^{-1}) on the perchlorate concentration for Al and its three alloys at 25°C and at a current density of 0.10 mA cm^{-2} . (1) Al; (2) (Al + 6% Si) alloy; (3) (Al + 12% Si) alloy; (4) (Al + 18% Si) alloy

3.2.2. Effect of Applied Anodic Current Density

In order to gain more insight on the kinetics of passive layer growth and its breakdown by aggressive perchlorate ions, chronopotentiometry potential/time measurements for the four tested Al samples in 0.50 M NaClO₄ solution were performed at 25 °C under the influence of different applied current densities. Figure 10, as an example, represents *E/t* transients recorded for (Al + 12%Si) alloy. Similar plots were obtained for the other samples. It can be seen that an increase in *j_a* enhances the rate of film growth, shifts *E_b* towards more noble potentials and decreases *t_i*. The positive shift observed in *E_b* with increasing *j_a* could be explained on the basis that increasing *j_a* results in an enhancement in the rate of O₂⁻ ion transport across the pre-existing oxide film toward the metal/oxide interface, where the growth of the oxide film takes place [13]. An increase in current density enhances the electric field across the oxide film, and therefore increases the rate of ion transport. Thus, the rate of passive layer growth is increased. This increase in the rate of passive layer growth with increasing *j_a* causes the potential to move towards more positive values to commence passivity breakdown and initiate pitting corrosion. This may explain the positive shift of *E_b* with increasing current density.

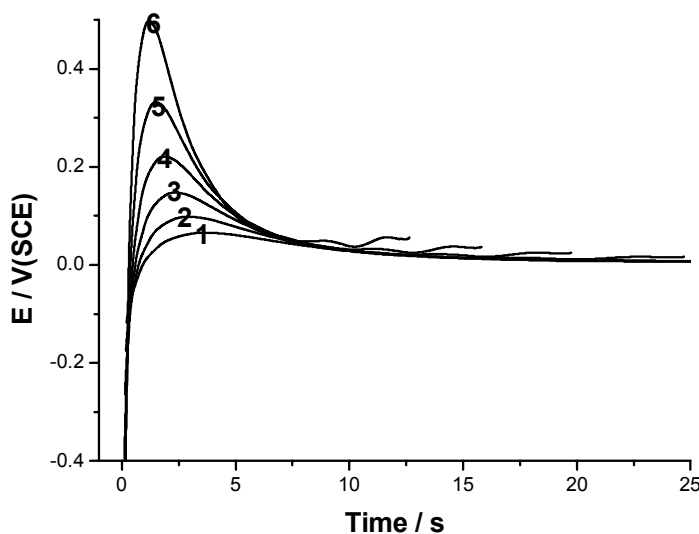


Figure 10. Potential/time transients recorded for pure Al in 0.50 M NaClO₄ solution at 25 °C and at different current densities. (1) 0.05 mA cm⁻²; (2) 0.10 mA cm⁻²; (3) 0.20 mA cm⁻²; (4) 0.30 mA cm⁻²; (5) 0.40 mA cm⁻²; (6) 0.50 mA cm⁻²

3.2.3. Effect of Inorganic Inhibitors

The goal of this section is twofold. Firstly, to gain more information on the role of tungstates and molybdates, as inorganic inhibitors, on the pitting corrosion inhibition of the four tested Al samples in perchlorate solutions. Secondly, to confirm the results obtained from polarization measurements. In the present work, the effect of adding increasing concentrations of MoO₄²⁻ and WO₄²⁻ ions on the potential/time transients of the four tested Al samples in 0.50 M NaClO₄ solution at 25 °C and at *j_a* = 0.10 mA cm⁻² has been studied. Some of the obtained results are depicted in Figures 11 and 12. It follows from the data of Figure 11 and Figure 12 that the addition of either MoO₄²⁻ or WO₄²⁻ ions into the perchlorate solution shifts *E_b* to more noble direction and increases the incubation time, reflecting the inhibition function of these anions [26]. These results support findings obtained from polarization measurements (see Section 3.1.6). As previously discussed, there is a competitive adsorption between these two inorganic inhibitor anions, namely (MoO₄²⁻ and WO₄²⁻ anions) and the aggressive ClO₄⁻ anions on the surface of the passive layer. These inhibitor anions, due to their specific adsorbability, can displace ClO₄⁻ anions from their preferential adsorption sites. Consequently, the rate of passive layer growth in perchlorate solutions containing these inhibitor anions is high compared with in solution containing ClO₄⁻ anions only. Moreover, the incorporation of the reduction products of these inhibitors (MoO₂ and WO₂) in the passive layer will offer better protective properties against the aggressiveness of ClO₄⁻ ions towards the passive layer [26].

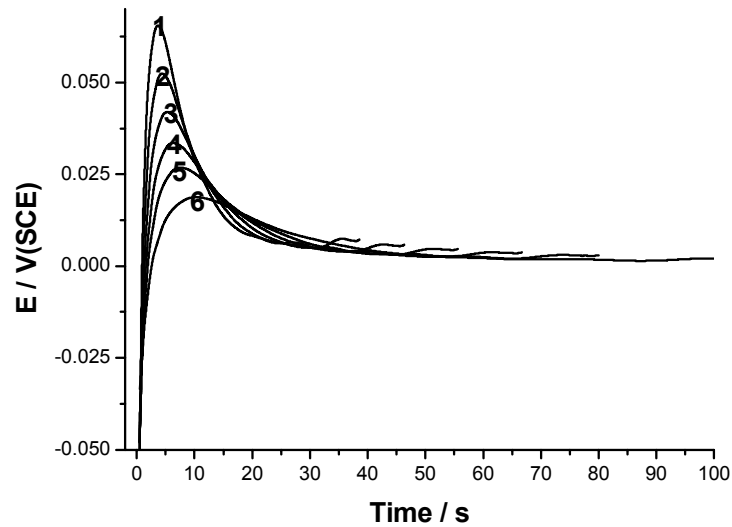


Figure 11. Potential/time curves of Al in 0.50 M NaClO₄ solution in the absence and presence of various concentrations (0.001 – 0.01) of Na₂MoO₄ at a current density of 0.10 mA cm⁻² and at 25 °C. (1) Blank; (2) 0.001 M; (3) 0.002 M; (4) 0.004 M; (5) 0.008 M; (6) 0.01 M

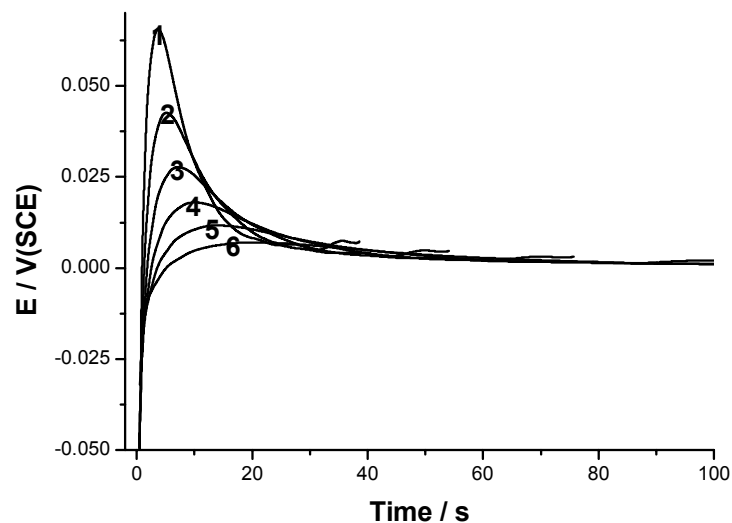


Figure 12. Potential/time curves of Al in 0.50 M NaClO₄ solution in the absence and presence of various concentrations (0.001 – 0.01) of Na₂WO₄ at a current density of 0.10 mA cm⁻² and at 25 °C. (1) Blank; (2) 0.001 M; (3) 0.002 M; (4) 0.004 M; (5) 0.008 M; (6) 0.01 M

3.3. Surface Analysis of the Passive Oxide Film Using EDX

To clarify the adsorption of the two inorganic inhibitor anions on the electrode surface and the incorporation of their reduction products in the passive layer, the EDX examination system was adopted. The electrode surface has been investigated for pure Al in 0.50 M perchlorate solutions (Figure 13(a)) and some investigation was made in the presence of 0.05 M MoO₄²⁻ and WO₄²⁻ anions (Figures 13(b) and 13(c), respectively). The EDX spectra presented in Figure 13 show clear and sharp signals characteristic of Al and O. This result demonstrates that the passive layer formed on the surface of Al in 0.50 M NaClO₄ solution may be Al₂O₃. On the other hand, the EDX spectra recorded for Al in 0.50 M NaClO₄ solution containing 0.05 M MoO₄²⁻ and WO₄²⁻ anions showed additional signals characteristic for Mo and W, respectively. In addition the O signal has been found to be enhanced.

It is possible that MoO₂ and WO₂ (the reduced form of molybdate and tungstenate anions) become part of the passive oxide film, and this may explain the remarkable increase in the O signal compared with that observed in perchlorate free solution (see Figure 13(a)). The incorporated MoO₂ and WO₂ oxides tend to plug its pores and flaws,

thereby imparting to it better protective properties. These results clearly demonstrate that the inhibition influence of MoO_4^{2-} and WO_4^{2-} anions is due to the formation of both MoO_2 and WO_2 in the passive oxide film.

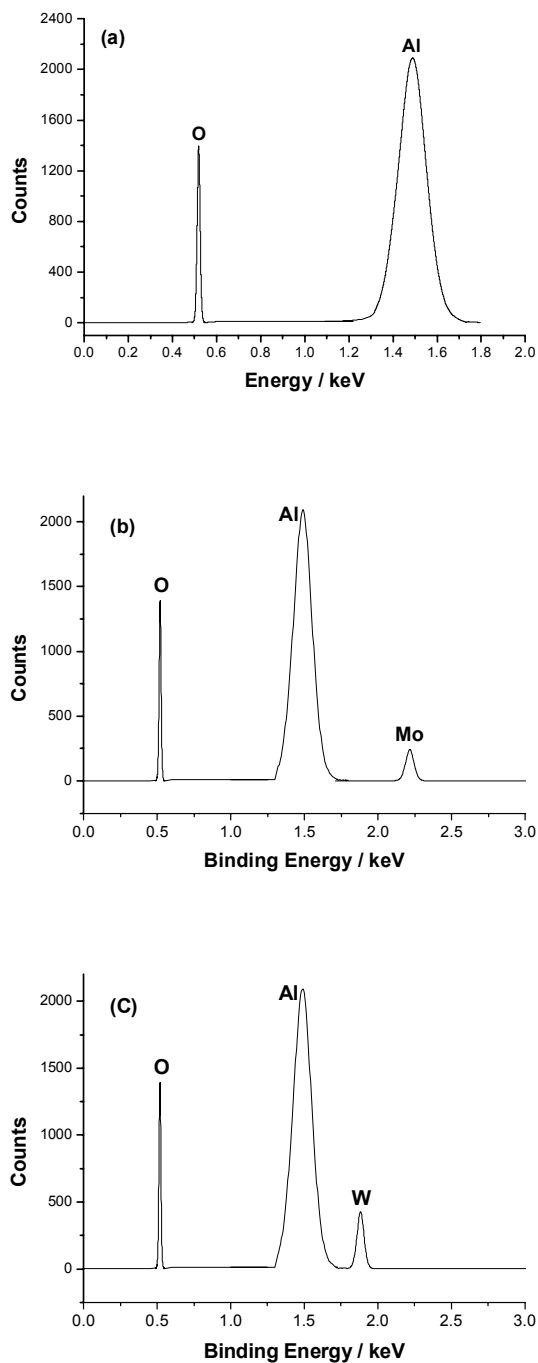


Figure 13. EDX spectra recorded for Al under potentiostatic regime at a given potential within the potential range of the passive region and at 25 °C in: (a) 0.50 M NaClO₄ only, (b) (0.50 M NaClO₄ + 0.05 M Na₂MoO₄), (c) (0.50 M NaClO₄ + 0.05 M Na₂WO₄)

4. CONCLUSIONS

1. The pitting corrosion of Al, (Al + 6%Si), (Al + 12%Si) and (Al + 18%Si) in NaClO₄ solutions free from and containing WO₄²⁻ and MoO₄²⁻ ions was examined using potentiodynamic polarization and galvanostatic measurements.
2. In perchlorate solution, the potentiodynamic anodic polarization curves, recorded for the four samples, do not exhibit active dissolution region due to spontaneous passivation. Passivity is due to the presence of an Al₂O₃ film on the electrode surface.
3. The pitting corrosion of Al increases with increasing ClO₄⁻ concentration, while it decreases with increasing Si content in the alloy.
4. Addition of WO₄²⁻ and MoO₄²⁻ ions to perchlorate solutions inhibits pitting corrosion of all samples.
5. Galvanostatic measurements showed that an incubation time, t_i , is necessary before pit nucleation and growth to occur.
6. The rate of pit nucleation, t_i^{-1} , increases with increasing ClO₄⁻ concentration and applied anodic current density, but decreases with increasing percentage of Si in the alloy.

ACKNOWLEDGMENT

The author wishes to thank Prince Sultan Bin Abdulaziz Al-Saud, First Deputy Premier, Minister of Defense and Aviation and Inspector General, and Prince Bandar Bin Sultan Bin Abdulaziz Al-Saud, the Secretary-General of the National Security Council, for their financial support for this project.

REFERENCES

- [1] K. Videm, "The Electrochemistry of Uniform Corrosion and Pitting of Aluminium", *Kjeller Report 62*. Kjeller, Norway: Institute for Atomenergi, 1974.
- [2] H.J.W. Lenderink, M.V.D. Linden, and J.H.W. DE Wit, "Corrosion of Aluminium in Acidic and Neutral Solutions", *Electrochim. Acta*, **38**(1993), p. 1989
- [3] C.M.A. Brett, "Inhibition of Aluminium Corrosion in Chloride Media: an Impedance Study", *Portug. Electrochim Acta*, **7**(1989), p. 123.
- [4] C.M.A. Brett, "The Application of Electrochemical Impedance Techniques to Aluminium Corrosion in Acidic Chloride Solution", *J. Appl. Electrochem.*, **20**(1990), p. 1000.
- [5] P.L. Cabot, F.A. Centellas, E. Perez, and R. Loukili, "Pitting and Repassivation Processes of Al-Zn-Mg Alloys in Chloride Solutions Containing Sulphate", *Electrochim. Acta*, **38** (1993), p. 2741
- [6] F.M. Al-Kharafi and W.A. Badawy, "Inhibition of Corrosion of Al 6061, Aluminum, and an Aluminum-Copper Alloy in Chloride-free Aqueous Media: Part 2 – Behavior in Basic Solutions", *Corros.*, **54** (1998), p. 377.
- [7] Joong-Do Kim and Su-IL Pyun, "Effects of Electrolyte Composition and Applied Potential on the Repassivation Kinetics of Pure Aluminium", *Electrochim. Acta.*, **40** (1995), p. 1863.
- [8] W.C. Moshier, G.D. Davis and J.S. Ahearn, "The Corrosion and Passivity of Aluminum Exposed to Dilute Sodium Sulfate Solutions", *Corros. Sci.*, **27** (1987), p. 785.
- [9] E. McCafferty, "A Competitive Adsorption Model for the Inhibition of Crevice Corrosion and Pitting", *J. Electrochem. Soc.*, **137** (1990), p. 3731.
- [10] A. Kolics, J.C. Polkinghorne, and A. Wieckowski, "Adsorption of Sulfate and Chloride Ions on Aluminum", *Electrochim. Acta*, **43** (1998), p. 3605.
- [11] H. Bohni and H.H. Uhlig, "Environmental Factors Affecting Critical Pitting Potential of Aluminum", *J. Electrochem. Soc.*, **116** (1969), p. 906.
- [12] H. Kaesche, *Z. Physik Chem. N.F.*, **34** (1962), p. 87.
- [13] Mohammed A. Amin, Sayed S. Abd El Rehim, and Essam E.F. El Sherbini, "AC and DC Studies of the Pitting Corrosion of Al in Perchlorate Solutions", *Electrochim. Acta*, **51** (2006), p. 4754.

- [14] G.G. Lang and G. Horanyi, "Some Interesting Aspects of the Catalytic and Electrocatalytic Reduction of Perchlorate Ions", *J. Electroanal. Chem.*, **552** (2003), p. 197.
- [15] A.R. Despic and V.P. Parkhutike, "Electrochemistry of Aluminium in Aqueous Solutions and Physics of its Anodic Oxide", in *Modern Aspects of Electrochemistry* (ed. J.O.M. Bockris, B.E. Conway and R.M. White), vol. 20. New York: Plenum Press, 1989, p. 397.
- [16] J. Kruger, in *Passivity and Its Breakdown on Iron and Iron Base Alloys*, USA–Japan Seminar, NACE, Houston, TX, 1976, p. 91.
- [17] R.T. Foley, "Pitting Corrosion of Aluminium Single Crystal in NaCl Solutions", *Corrosion*, **42**(1986), p. 277.
- [18] J. R. Galvele, in *Passivity of Metals* (ed. R. P. Frankenthal and J. Kruger). Princeton, NJ: The Electrochemical Society, Inc., 1978, p. 285.
- [19] B. G. Ateya and H. W. Pickering. Princeton, NJ: The Electrochemical Society, Inc., 1978, p. 350.
- [20] G.C. Wood and A.J. Brock, *Trans. Inst. Met. Fin.*, **44**(1966), p. 189.
- [21] H.H. Strehblow and C.J. Doherty, "Examination of Aluminum Copper-Films during Anodic-Oxidation .1. Corrosion Studies", *J. Electrochem. Soc.*, **125**(1978), p. 30.
- [22] S.M. Abd El Halim, "Initiation and Inhibition of Pitting Corrosion in Alkali Solutions Under Potentiostatic Polarization Conditions", *Werkst. Korros.*, **30**(1979), p. 631.
- [23] K.C. Emergul and A.A. Aksut, "The Effect of Sodium Molybdate on the Pitting Corrosion of Aluminum", *Corros. Sci.*, **45**(2003), p. 2415.
- [24] E. McCafferty, M.K. Berrett, and J.S. Murday, "An XPS Study of Passive Film Formation on Iron in Chromate Solutions", *Corros. Sci.*, **28** (1988), p. 559.
- [25] N. Xu, G.E. Thompson, J.L. Dawson, and G.C. Wood, "The Interaction of Chromate Species with Aluminium Supporting Anodic Films—I. Electronoptical Studies", *Corros. Sci.*, **34** (1993), p. 461.
- [26] M. Metikos-Hukovic, "Electrochemical Methods in the Study of Localized Corrosion Attack", *J. Appl. Electrochem.*, **22** (1992), p. 448.
- [27] H.H. Hassan, S.S. Abd El Rehim, and N.F. Mohamed, "Role of ClO_4^- in Breakdown of Tin Passivity in NaOH Solutions", *Corros. Sci.*, **44** (2002), p. 37.
- [28] L.A. Ammar, S. Darwish, M. W. Khalil, and S. El Taher, "Anodic Oxide Film Formation on Tin", *Corrosion*, **46** (1990), p. 197.
- [29] E.E. Abd El Aal, "Effect of Cl^- Anions on Zinc Passivity in Borate Solution", *Corros. Sci.*, **42** (2000), p. 1.